Disabling ErbB Receptors with Rationally Designed Exocyclic Mimetics of Antibodies: Structure−Function Analysis[†]

Alan Berezov, Hong-Tao Zhang, Mark I. Greene,* and Ramachandran Murali*

Department of Pathology and Laboratory Medicine, University of Pennsylvania School of Medicine, 36th and Hamilton Walk, Philadelphia, Pennsylvania 19104

Overexpression of the HER2 receptor is observed in about 30% of breast and ovarian cancers and is often associated with an unfavorable prognosis. We have recently designed an anti-HER2 peptide (AHNP) based on the structure of the CDR-H3 loop of the anti-HER2 rhumAb 4D5 and showed that this peptide can mimic some functions of rhumAb 4D5. The peptide disabled HER2 tyrosine kinases in vitro and in vivo similar to the monoclonal antibody (Park, B.-W. et al. *Nat. Biotechnol.* **2000,** *18,* 194−198). AHNP has been shown to selectively bind to the extracellular domain of the HER2 receptor with a submicromolar affinity in Biacore assays. In the present paper, we demonstrate that in addition to being a structural and functional mimic of rhumAb 4D5, AHNP can also effectively compete with the antibody for binding to the HER2 receptor indicating a similar binding site for the peptide and the parental antibody. To further develop AHNP as an antitumor agent useful for preclinical trials and as a radiopharmaceutical to be used for tumor imaging, a number of derivatives of AHNP have been designed. Structure−function relationships have been studied using surface plasmon resonance technology. Some of the AHNP analogues have improved binding properties, solubility, and cytotoxic activity relative to AHNP. Residues in the exocyclic region of AHNP appear to be essential for high-affinity binding. Kinetic and equilibrium analysis of peptide-receptor binding for various AHNP analogues revealed a strong correlation between peptide binding characteristics and their biological activity. For AHNP analogues, dissociation rate constants have been shown to be better indicators of peptide biological activity than receptor-binding affinities. This study demonstrates a possibility of mimicking the well-documented antibody effects and its applications in tumor therapy by much smaller antibody-based cyclic peptides with potentially significant therapeutic advantages. Strategies used to improve binding properties of rationally designed AHNP analogues are discussed.

Introduction

HER2 (neu, c-erbB2) is a member of the epidermal growth factor (EGFR)[1] or HER family of tyrosine kinase receptors that also includes HER1 (EGFR, c-erbB1, HER3 (c-erbB3), and HER4 (c-erbB4).[1−4] Amplification of HER2 gene and overexpression of HER2 protein has been found in breast and ovarian cancers, as well as tumors of the lung, salivary gland, kidney, and bladder.[5] Greater expression of HER2 on transformed cells than on normal epithelial tissues allows selective targeting of tumor cells using various strategies.[6−14]

Recently, some progress has been made in the development of monoclonal antibody-based therapeutics targeting tumor cell surface antigens (see ref 15 for a recent review). The anti-HER2 antibody "trastuzumab" (Herceptin; Genentech, San Francisco) produces objective responses in some patients with advanced breast cancer showing overexpressed HER2 oncoprotein. The antibody has been shown to antagonize the constitutive growth-signaling properties of the HER2 system, enlist immune cells to attack and kill the tumor target, and augment chemotherapy-induced cytotoxicity.[16] Another important application of antibodies that has been extensively developed over the past two decades is tumor imaging by numerous anticancer antibodies against various molecular targets including breast cancer imaging.[17]

Application of intact antibody molecules as therapeutic or diagnostic molecules remains limited, since they may cause an immune response and have little tumor penetration and high background noise. One of the ways to overcome the limitation of therapeutic macromolecules is to develop a small molecule. A promising approach is to design small peptides derived from the antigen-binding site of antibodies. Historically, few therapeutic peptide products have been used in the clinic because of the difficulties with delivery, stability, and above all, with cost-effective and reliable peptide manufacture. However, recent progress in high quantity peptide synthesis, as well as in screening and optimization of peptide leads, has resulted in an explosion in the number of candidate peptides and a renewed interest in their commercial development.[18]

Since complementarity-determining regions (CDRs) of antibodies mediate their high affinity binding and specificity to antigens,[19] we proposed that peptide analogues of CDRs can be developed for antibodies with known sequences and structures.[20−24] Since our first studies in this area,[20,21] the strategy of designing CDR-

* Correspondence should be addressed to R. M. (murali@xray.med.upenn.edu) or M.I.G. (greene@reo.med.upenn.edu). Tel.: 215-573-9256 (R.M.); 215-898-2847 (M.I.G.). FAX: 215-898-2401.

Table 1. Summary of Biophysical Properties and Biological Activities for AHNP Analogs

AHNP analogues	composition	$k_{on} \times 10^2$ M^{-1} s^{-1}	binding to HER2 $k_{off} \times 10^{-4}$ s^{-1}	K_D μM	% inhibition[a]	solubility[b]
1	FCDGFYACYMDV-NH2	14.10	4.53	0.32	35.5	limited
2	FCDGFYACYMDV-OH	9.90	6.43	0.65	22.3	limited
3	YCDGFYACYMDV-NH2	19.60	2.94	0.15	59.6	limited
4	dFCDGFYACdYMDV-NH2	17.20	6.03	0.35	26.0	good
5	FCDGFYACYMDVK-NH2	6.17	5.12	0.83	20.0	limited
6	FCDGFYACYKDV-OH	2.19	12.50	5.70	8.4	good
7	GFCDGFYACYMDV-OH	11.10	8.08	0.73	15.8	good
8	FCGDGFYACYMDV-OH	9.22	7.01	0.76	18.4	good
9	FCDGFYACYMDV-OH	2.98	10.60	3.56	12.8	good

[a] Inhibition of T6−17 cell proliferation in MTT assays. Each value represents an average of at least four samples. Standard error did not exceed 5% for any of the studied analogues. [b] Peptide solubility is indicated as good if the peptide can be readily dissolved in the PBS buffer at 1 mg/mL, and as limited if pH adjustment is required for dissolving the peptide.

based mimetics has been widely used by other investigators in rational drug design.[25−39] Although many of the reported peptides display highly specific antigen binding similar to the parental antibody, their antigen-binding affinity is in most cases substantially lower.

Recently, we have reported the design of an anti-HER2 peptide mimetic (AHNP, peptide (**1**), Table 1) derived from the structure of the CDR-H3 loop of the anti-HER2 rhumAb 4D5, and demonstrated its in vitro and in vivo activities in disabling HER2 tyrosine kinases similar to the monoclonal antibody.[40]

Binding of AHNP has been studied by means of surface plasmon resonance (Biacore) technology. In Biacore experiments, one of the interacting molecules (termed the ligand) is immobilized on the sensor surface, and the other interactant (termed the analyte) is continuously flown over that surface in a micro-flow cell. The interaction between the ligand and the analyte are monitored using a light source that is reflected at the immobilized chip. Binding of the analyte to the immobilized ligand changes the resonance angle of the reflected light due to changes in the refractive index of the surface. The response is plotted in real time in the form of sensorgram curves. The advantage with this approach is its sensitivity, ease of use, and ability to perform experiments with few microgram quantities of proteins and peptides. In addition, the kinetic binding studies reveal association and disassociation rates of the analyte which may be more relevant for understanding the pharmocokinetics of drug-receptor interactions.

A typical sensorgram for AHNP binding to the HER2 receptor is shown in Figure 1. Kinetic constants were estimated by global fitting analysis of the titration curves to the 1:1 Langmurian interaction model, which gave a k_{on} of 1.41×10^3 M^{-1} s^{-1}, and a k_{off} of 4.53×10^{-4} s^{-1}. The k_{off}/k_{on} ratio gave a value of 0.32 μM for the dissociation constant (K_D). The curves shown in Figure 1 were calculated from the experimentally observed curves by successive subtractions of signals obtained for the reference surface and averaged signals for the running buffer injected under the same conditions as the tested peptide.[41−44] Good fitting of experimental data to the calculated curves has been observed, suggesting a simple pseudo-first-order interaction between the peptide and the receptor.

In the present study, we report a rational design and structure−function analysis of AHNP analogues with improved pharmacological features that could be used as antitumor agents and developed into radiopharmaceuticals.
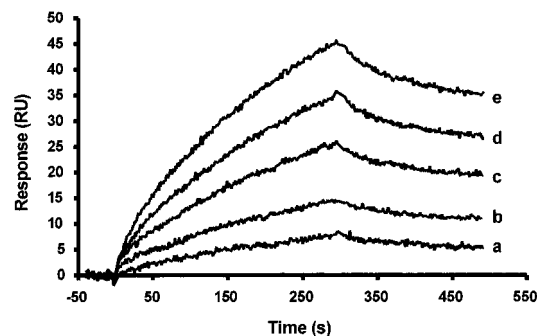

Figure 1. Biosensor dose dependence curves for binding of AHNP to the immobilized HER2 receptor. AHNP was injected at 0.5 μM (a), 1 μM (b), 2 μM (c), 4 μM (d), and 8 μM (e) concentrations at a flow rate of 20 μL/min. Sensorgrams show binding of AHNP to the immobilized HER2 (first 300 s) followed by the peptide dissociation from the receptor surface (last 240 s).

Results

In the present study, a number of anti-HER2/neu peptide mimetic (AHNP) analogues have been engineered into better therapeutic agents in terms of their binding properties, specificity, and solubility. We have also explored the ways to incorporate a reactive amino group to conjugate fluorescent and positron emission tomography (PET) agents[45] and studied its effect on binding to the receptor.

Competition Studies. Earlier, we have shown that the AHNP peptide can mimic some functions of the anti-HER2/neu antibody, rhumAb 4D5 in vitro and in vivo.[40] In the present study, we have analyzed the structural mimicry of rhumAb 4D5 by AHNP in terms of binding to the HER2 receptor by means of competition binding studies between AHNP and the parental antibody. To that end, injections of AHNP at variable concentrations (from 0 to 90 μM) were followed by injections of rhumAb 4D5 at a constant 1 nM concentration, using the "Coinject" mode of the Biacore instrument. Increase in the amount of preinjected AHNP resulted in a steady inhibition of the antibody binding (Figure 2) with an apparent IC$_{50}$ of 3.4 μM, indicating overlapping binding sites for AHNP and rhumAb 4D5 on the surface of HER2.

Design of AHNP Analogues. A number of modifications have been introduced to the sequence of the AHNP peptide to improve its receptor binding and solubility, properties that are important for both major applications: as a therapeutic and as a tumor imaging agent. For the PET studies, we are planning to attach ^{18}F and
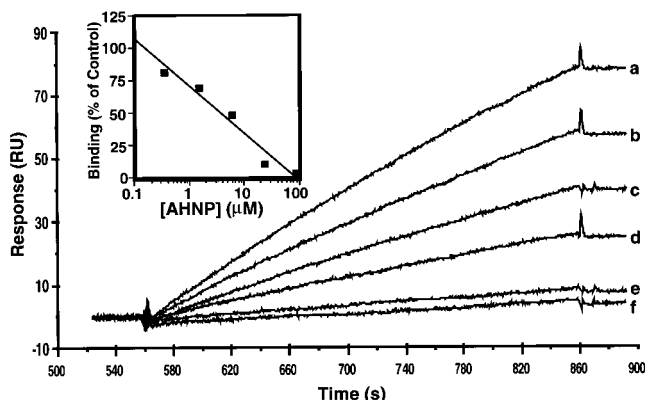
Figure 2. Biacore analysis of the inhibitory effect of AHNP on rhumAb 4D5 binding to immobilized HER2. Sensorgrams show binding of 1 nM rhumAb 4D5 to HER2 after preinjection of 0 μM (a), 0.35 μM (b), 1.4 μM (c), 5.6 μM (d), 22 μM (e), and 89 μM (f) AHNP. Inset shows correlation between the initial rate of rhumAb 4D5 binding to HER2 and concentration of preinjected AHNP.

[90]Y via an α- or ϵ-amine group of AHNP.[45] Thus, it is necessary to improve AHNP by either increasing the accessibility of the N-terminal residue or by introducing a Lys residue, which could be readily labeled without diminishing the binding affinity. Two types of changes have been made: (1) addition of polar groups, and (2) mutation of Met to Lys and introduction of D-isomers at the termini. Most of the changes in AHNP were restricted to the N- and C-terminal residues outside the loop constrained by the disulfide bond to preserve the binding nature of AHNP.

Chronologically, peptide **8** was the first AHNP analogue that we designed based on the structures of monoclonal antibodies 4D5 and its rat homologue 7.16. To increase rigidity of the cyclic peptide, we have designed **2** in which one of the β-turn forming Gly residue has been deleted.[40] Three other analogues have been designed to analyze effects of different substitutions on biological activity, binding properties, and solubility. An AHNP peptide has been designed based on the structure of **2** by replacing the C-terminal carboxylate by an amide group. In **3**, the N-terminal Phe of the AHNP peptide has been replaced with Tyr, and in **4**, aromatic residues positioned before and after the disulfide bond were replaced with their D-amino acid optical isomers. A Lys residue has been included in the sequence of peptide **2** by either replacing Met (resulting in the **6** analog) or by placing it as a C-terminal residue (**5**).

The designed AHNP analogue peptides have been synthesized, cyclized (except for peptide **9** used as a control), and tested for binding to HER2, biological activity in an MTT assay, and solubility (Table 1). Binding constants including the association (k_{on}) and dissociation (k_{off}) rate constants, and the equilibrium dissociation constant (K_D) shown in Table 1 were determined by analyzing dose dependence curves obtained for each AHNP analogue in a similar fashion as described for AHNP (data not shown). Effects of different substitutions/additions in AHNP sequence on receptor binding, biological activity, and solubility are summarized in Table 1.

Kinetic Binding Analysis of the AHNP Analogues. Biacore analysis of interactions between AHNP

analogues and immobilized HER2 has been performed to test effects of the introduced sequence modifications on the binding affinity and kinetic constants for each peptide. Cyclization is known to be an efficient way of constraining peptides in a binding-competent conformation. Consistent with that, the affinity of cyclic peptide **2** for HER2 was more than 5-fold higher than that of the linear analogue **9** (Table 1). Restriction of the loop by deletion of one of the β-turn glycines (transition from **8** to **2**) also resulted in improvements in both affinity and dissociation kinetics. The effect of the charged C-terminal carboxylate group in **2** on binding properties has been tested by replacing it with an amide group in AHNP. Elimination of the charged group in the C-terminal tail resulted in more than 2-fold increase in binding affinity. Similar, but even more dramatic loss of affinity occurred when Lys was introduced as a C-terminal residue in **5** (2.6-fold decrease) and especially when Lys was substituted for Met in **6** (8.8-fold decrease). In the latter case, in addition to the detrimental effect of the C-terminal hydroxyl group, a charged Lys residue replaces a hydrophobic Met residue, which may be important for binding (see discussion). In contrast, significant improvement in binding (more than 2-fold) has been achieved by introducing a polar hydroxyl group in the N-terminal residue by replacing Phe with Tyr in **3**. This peptide also had the lowest dissociation rate constant (k_{off}) among all tested AHNP analogues (2.94×10^{-4} s^{-1}), which is comparable with the k_{off} of 1.23×10^{-4} s^{-1} observed for rhumAb 4D5.[40]

Solubility. Four peptides listed in Table 1, **9**, **8**, **6**, and **4** have been shown to have a much higher solubility than the rest of the tested peptides (Table 1). These peptides could be readily dissolved in the PBS buffer, pH 7.4, at 1 mg/mL concentration without adjustment of pH. Good solubility has also been observed for the linear form of all tested peptides (data not shown). In contrast, all other tested peptides had a limited solubility at 1 mg/mL.

Biological Activity of the AHNP Analogues. Biological activity of AHNP analogues has been evaluated by their ability to inhibit cell proliferation using standard 3,(4,5-dimethylthiazol-2-yl)2,5-diphenyl-tetrazolium bromide) (MTT) assays.[46] HER2-expressing transformed tumor cells (T6-17) were used for this purpose.[40] In MTT assays, AHNP inhibited the growth of T6-17 cells, overexpressing transformed cell line, dose-dependently at concentrations ranging from 0.01 to 10 μg/mL. Biological activity of AHNP analogues is shown in Table 1. Each value represents an average of at least four samples. Standard error did not exceed 5% for any of the studied analogues. A wide range of activities has been observed for different peptides depending on the nature of introduced modifications. Analogue **3**, which has an enhanced receptor-binding affinity ($K_D = 150$ nM), was also the most active peptide in the MTT assay, showing almost twice the activity of AHNP (Table 1).

Accessibility of the N-Terminal Amino Group for Labeling. Since AHNP analogues can selectively bind to the oncogenic HER2 receptor, which is overexpressed in many different forms of cancer, fluorescently or radiolabeled AHNP derivatives could be potentially used as tumor imaging agents. Therefore, one of the
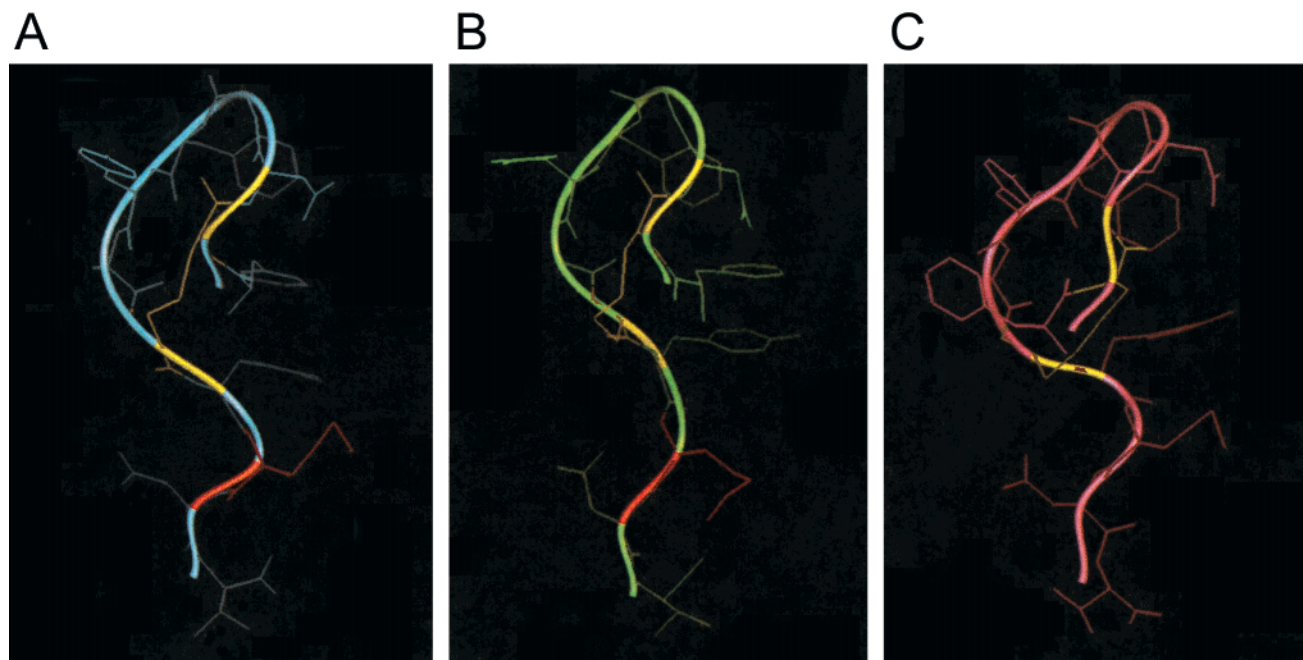
Figure 3. Molecular models of AHNP analogues. AHNP (A), **6** (B), and **8** (C). Cys residues forming the disulfide bond are shown in yellow. The Met residue in the tail region of AHNP (A) and the Lys residue replacing Met in **6** (B) are shown in red.

goals of our study was to obtain AHNP analogues that could be easily modified. Accessibility of different N-terminal or Lys amino groups for labeling with FITC was estimated by the HPLC analysis of the peptide-FITC reaction mixture as described in Experimental Procedures. In our preliminary studies, we found that the N-terminal amino group of AHNP has a very limited accessibility for fluorescent labeling by FITC (about 2−5% of the theoretically expected yield). To develop AHNP into a radiopharmaceutical we need to design an active AHNP analogue containing a reactive amino group. FITC labeling studies revealed that the N-terminal amino group of AHNP may be inaccessible for labeling. On the basis of the molecular model, it appears that the N-terminal aromatic residue buried in the hydrophobic core (Figure 3A) may hinder access of the bulky molecule, FITC. To overcome this problem, we decided to place a more flexible Gly residue at the N-terminus just before Phe1 (**7**). However, this also did not significantly improve the degree of labeling (7−10% yield), suggesting that steric hindrance may still be a factor. Further molecular modeling studies showed that **7** can adopt two main low-energy conformations with different orientations of the N-terminal Gly (Figure 4). In one of the conformational states, the N-terminus was oriented outside the ring created by the disulfide bond and was therefore solvent-exposed (Figure 4A). However, in the second conformation, Gly was oriented toward the inside of the ring and was buried between the ring residues (Figure 4B). Obviously, the second conformational state may be predominant in solution for **7**, which may explain its poor accessibility. Also, since Gly in the second conformational state is positioned very close to the disulfide bond, it is likely to interfere with peptide cyclization. This may account for an unusually slow cyclization rate that has been observed for **7** relative to other analogues. Cyclization half-time for **7** (about 6 days) is about 3-fold longer than a typical half-time, observed for **2** and other analogues.

Insertion of Gly inside the ring weakened the hydrophobic core leading to an increased solubility of **7** (Table 1). As expected, both Lys-containing peptides, **6** and **5**, were completely accessible for labeling showing almost qualitative reactivity of their ϵ-amino groups with FITC. Preliminary binding data obtained with FITC-modified **5** indicate that it has a receptor-binding affinity similar to the unlabeled peptide **5** (data not shown).

Discussion

Surface plasmon resonance analysis was our method of choice for characterization of peptide-receptor binding, since we were interested in obtaining not only equilibrium data, but also kinetic parameters of the interactions (for reasons discussed below). Because of the large number of tested peptides, the only practical way for screening was immobilization of HER2 on the chip and injection of peptides as soluble analytes. Although direct detection of analytes smaller than 5000 Da was once considered unfeasible with standard Biacore protocols,[47,48] recent advances in the technology, such as higher sensitivity and improved microfluidics, have enabled development of direct binding assays between immobilized proteins and low-molecular-weight analytes including peptides[44,49−51] and organic compounds.[52−58] Reproducible data with a high signal-to-noise ratio have been reported even though the change in molecular mass upon analyte binding was in some cases as low as 1%.[55,58] In some instances, modifying experimental conditions by using very dense ligand surfaces and/or high peptide concentrations with high flow rates was critical for obtaining good signal-to-noise ratios.[49,50] Accuracy of experiments with low signal levels can be improved by increasing the number of collected data points, increasing analyte concentration, and signal averaging of data derived from repeat sensorgrams.[44] In our Biacore studies of low-molecular-weight cyclic peptides, highly reproducible signals could
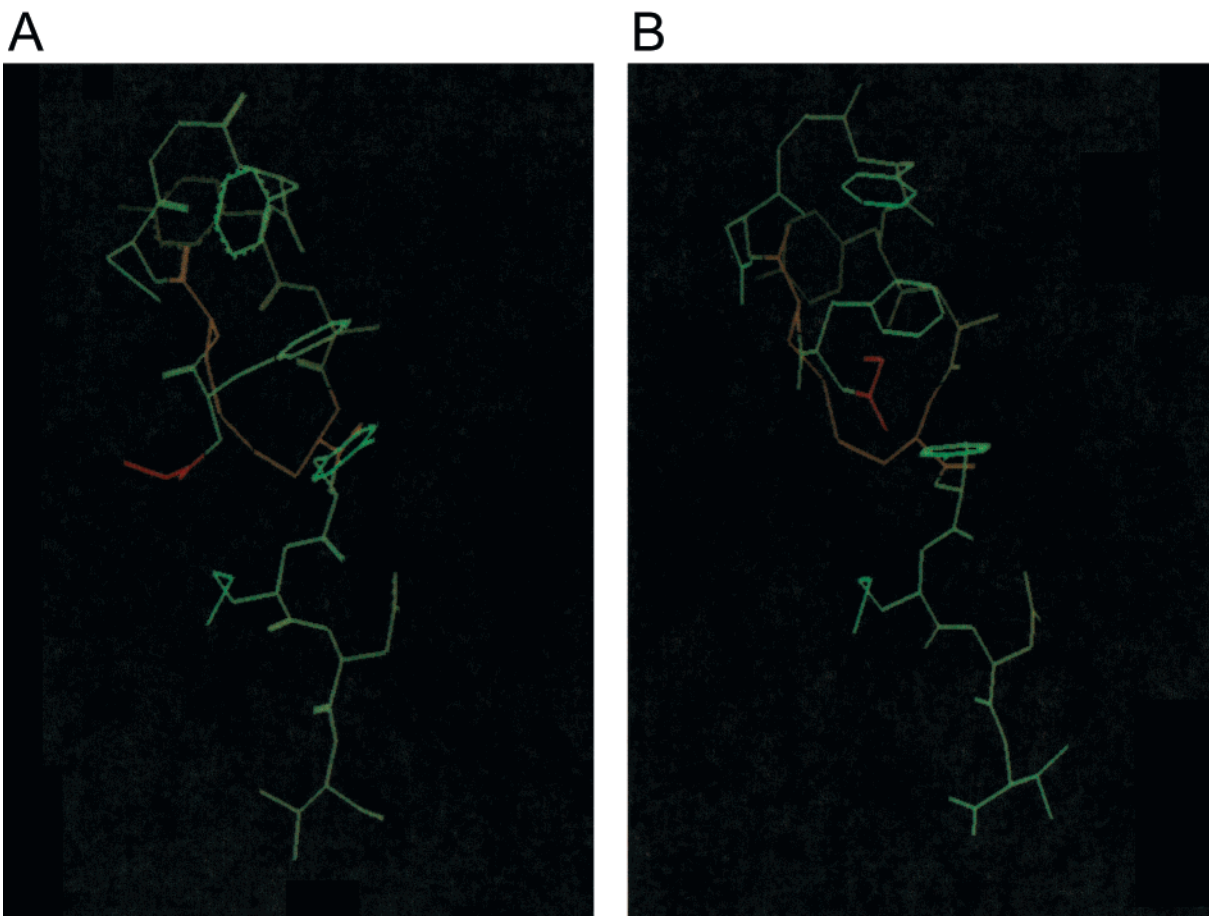
Figure 4. Low-energy conformers of **7**. Molecular models of two low-energy conformers of **7** with the solvent-exposed (A) and buried (B) orientation of the N-terminal Gly. The Gly residue is colored red.

be obtained after double corrections of data for the reference surface and the running buffer signals.

A large number of antibody-derived peptides have been reported, yet remarkably few of them have been demonstrated to mimic the parental mAb in terms of structure and function. Here we showed that AHNP not only induce antitumor effects such as its parent antibody, but also share binding epitope on the HER2 receptor. This information is very important, since peptides are usually designed to mimic antigen-binding properties and therapeutic effects of corresponding mAbs. Although peptide mimetics that bind to receptors are often presumed to be direct structural analogues of the loops that they mimic, and are therefore expected to have the same binding sites as the loops, this is not always an obvious fact and has to be proven experimentally. It has been shown that some peptide mimetics designed to mimic enzyme substrates and even some natural enzyme inhibitors do not bind in a substrate-like manner.[59-63] For a large number of receptors, analysis of the endogenous peptide and antagonists' binding sites by site-directed mutagenesis indicated that antagonists and the parent peptide bind to different subsites.[64-66] Backward binding is a common occurrence, which has been exploited to develop novel inhibitors.[59,60,67]

Although we have shown that AHNP and rhumAb 4D5 interact with the same binding site on the HER2 surface, it appears that the nature of receptor interaction with the peptide and the antibody are quite different. Analysis of surface regeneration conditions that are efficient (or necessary) for the destruction of a ligand–analyte complex can help provide insight into the major forces involved in the complex formation. In the rhumAb 4D5-HER2 complex, electrostatic interactions seem to play a predominant role, since the antibody could be easily washed off the receptor surface by high salt concentrations (4.5 M $MgCl_2$), but was resistant to treatment with either detergent (0.2% SDS) or a mixture of organic solvents. In contrast, the AHNP–HER2 complex was resistant to salt, but readily dissociated upon addition of either detergent or organic solvents, suggesting the involvement of hydrophobic interactions in complex stability. Obviously, aromatic residues at both sides of the disulfide bond, as well as the hydrophobic residues in the tail of AHNP and its analogues, contribute significantly to the overall energy of binding, since substitution or modification of these residues adversely affects the binding affinity (Table 1). Moreover, it is clear that for the AHNP peptide, in addition to the binding forces inherited from the CDR3 loop of rhumAb 4D5, which obviously direct the peptide to bind to the CDR3 epitope on the receptor surface, some new complex-stabilizing hydrophobic bonds are formed between the peptide and receptor, which are absent in the parent antibody.

Poor solubility of peptidomimetics often limits their usefulness as therapeutic agents. We have improved the solubility of some AHNP analogues without further loss of the binding characteristics. Molecular modeling was
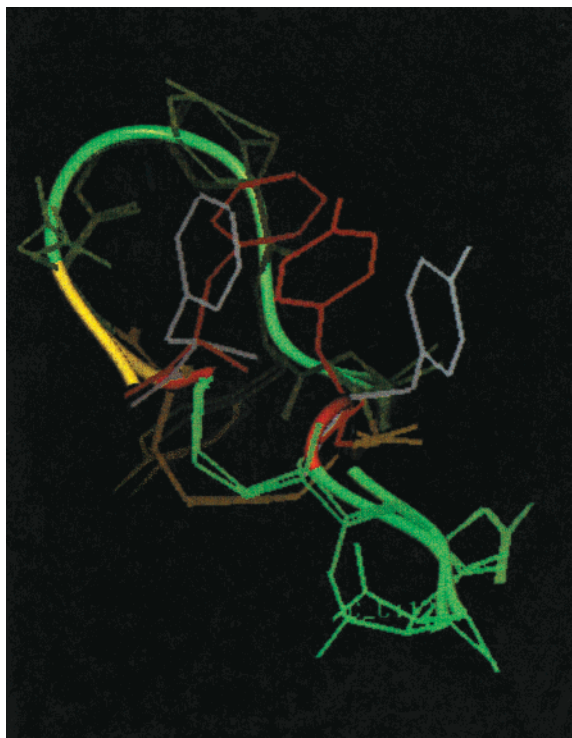
Figure 5. Molecular model of **4** superimposed with AHNP. Aromatic side chains at both ends of the disulfide bond are colored red for AHNP and white for **4**.

used to understand the effect of mutations on solubility. Molecular modeling of AHNP showed formation of a hydrophobic core by Phe1, Cys2, Phe5, Ala7, Cys8, Tyr9, and Met10 residues upon peptide cyclization (Figure 3A). Increasing backbone flexibility by adding one more Gly residue (**8**) enhanced spatial separation and mobility of the hydrophobic residues which may have resulted in the improved solubility. Replacement of Met10 with Lys in **6** improves solubility by reducing the size of the hydrophobic core (Figure 3B). Phe1 and Tyr9 at the termini of AHNP form the center of the core. Replacement of these residues by their D-isomers increases the separation between them by changing the orientation of the aromatic side chains relative to each other (Figure 5), which leads to the increased solubility. Interestingly, when polar groups were introduced in residues outside the hydrophobic core (in **2** and **5**), no improvement in

solubility has been observed (Table 1), confirming a critical role played by the hydrophobic core in peptide solubility. Another analogue that displayed a good solubility is **7**.

Balancing hydrophilicity and hydrophobicity is critical for high affinity binding, especially for small molecules. In this study, we have tested effects of different sequence modifications in the AHNP analogues on their biological activity and binding properties. Interestingly, the C-terminal tail region of the studied peptides was found to play an important role in receptor binding. In antigen−antibody complexes, the CDR loops and framework regions immediately after the CDR loops have been reported to be critical for antigen binding.[36,37,68,69] However, it is not clear how residues from the framework proximal to CDR can play a critical role in binding.

The C-terminal Met, Asp, and Val residues in AHNP analogues are derived from the framework region of anti-HER2 antibodies. Replacement of the Met residue in the tail with Lys (**6**) resulted in a dramatic decrease in binding affinity by about 1 order of magnitude (Table 1). The effect of addition of a Lys residue following the tail sequence **5** on receptor binding affinity was less dramatic but also significant (2.5-fold decrease, Table 1). Molecular modeling of the AHNP peptide revealed that the Met residue and aromatic residues form a hydrophobic core (Figure 3A). This formation of the hydrophobic core may be critical for receptor binding, having either enthalpic (formation of hydrophobic bonds with receptor residues) or entropic (constraining the peptide in an active conformation) effects, or both. The Met residue is a part of the core and may also be important for its integrity, which is consistent with the observed improvement in aqueous solubility of **6** relative to **2** (Table 1). These observations suggest that additional interactions of the C-terminal tail residues of the AHNP analogues with the receptor may be partly compensating for the diminished interface area in the peptide−receptor complex relative to the antibody−receptor complex.

Structure−activity relationship has been studied for the whole series of peptides. Cell growth inhibition activities obtained in the MTT assays for each analogue were plotted versus their affinity for HER2, estimated in the surface plasmon resonance study (Figure 6A). A
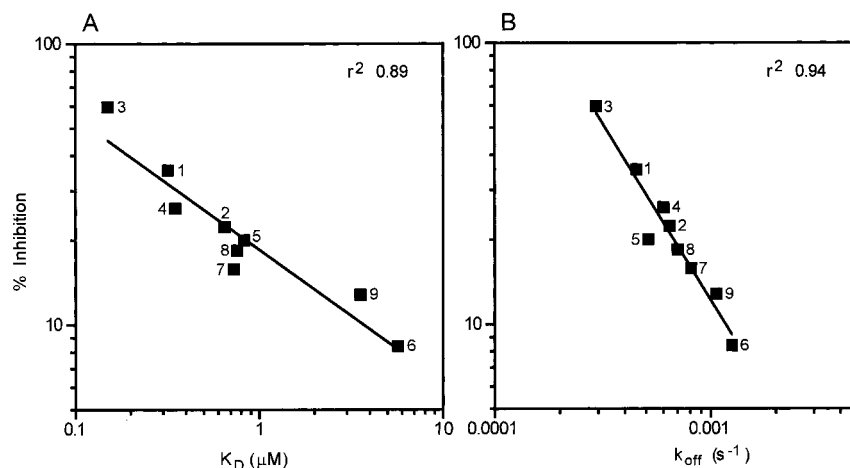
Figure 6. Structure−function analysis of AHNP analogues. Plots show correlation between peptides' activities in MTT assays and (A) their receptor binding affinities, or (B) dissociation rate constants obtained in Biacore studies.

strong correlation ($r^2 = 0.89$) has been determined between the peptides' receptor affinities and their inhibitory effects, suggesting that the observed biological activities are mediated by binding to HER2. As expected, the most active peptide (**3**) had the highest binding affinity, while the affinity of the least active (**6**) was the lowest among all analogues. Although the overall correlation was rather strong, some notable deviations from the straight line have been observed. Thus **2** and **7** peptides have a relatively small (12%) difference in affinities, but much more pronounced difference (41%) in inhibition. Similar discrepancies have been detected by comparing AHNP with **4** (9% difference in affinity versus 35% difference in inhibitory effect). The biggest inconsistency has been observed for the **7** and **5** pair. Although **5** is 27% more active, it binds to the receptor with a 14% lower affinity than **7** (Table 1).

To test whether these discrepancies could be explained by differences in the kinetic rate constants, activity data were plotted against the dissociation rate constants (k_{off}) observed in Biacore assays (Figure 6B). Remarkably, inhibitory activity showed an even stronger correlation with the k_{off} ($r^2 = 0.94$), than with the K_D. Comparison of the two plots (Figure 6A,B) suggests that stronger inhibitory activity observed for AHNP, **2**, and **5** can be better explained by their slow dissociation rates rather than by their high receptor-binding affinities.

Analysis of the drug-receptor dissociation rate is essential for a proper design and interpretation of receptor-binding studies, as well as for the selection of drug candidates.[70,71] For slowly dissociating drugs, binding equilibrium cannot be reached in short-incubation time experiments, thus preventing competitive inhibition. A slow dissociation rate has been shown to play an important role for the biological activity of the drug.[55,70] Since rapidly dissociating drugs can reach a competitive binding equilibrium with the endogenous receptor ligands, they are easily displaced from the receptor sites by increased concentrations of the ligands, which in most cases have higher receptor-binding affinities than the drugs. However, slowly dissociating drugs form inactive receptor−drug complexes which have very long half-lives. Even if the overall binding affinity is low because of a slow association rate, these drugs can provoke a permanent receptor blockade, which cannot be displaced by the endogenous ligands, thus acting as almost nonreversible antagonists. Dissociation rate might play an important role in long-term effects of drugs.[70] Therefore, analysis based on K_D values alone, could overlook potentially strong inhibitors that have slow binding and slow dissociation rates.[72] We have demonstrated that rhumAb 4D5 has about 2 orders of magnitude higher receptor-binding affinity than the AHNP peptides (Table 1). However, this difference is mostly due to a faster on-rate (higher k_{on}) of the antibody. In terms of the dissociation rate constant k_{off}, receptor-binding properties of the optimized peptides are very similar to those of the antibody. Although a big excess of AHNP is required to inhibit rhumAb 4D5−HER2 interaction (because of the difference in the binding affinity), the optimized peptides and the antibody have comparable biological activities in the MTT

assay,[40] in line with our observation that k_{off}, rather than K_D, determines the biological activity of the AHNP peptides.

Our studies showed the importance of the dissociation rate constant for biological activity of AHNP analogues. For this series of peptides, k_{off} has been shown to have a higher predictive value for the expected inhibitory effects than the dissociation constant (K_D) traditionally used for these purposes. Since AHNP analogues produce their biological effects by binding to HER2 and possibly inducing a conformational change that deactivates the receptor, our data indicate that increasing the half-life of the inactive peptide−receptor complexes is more efficient for the inhibition of normal receptor functioning than increasing the equilibrium concentration of these complexes.

Obviously, in the HER2 receptor system, AHNP peptides compete with some fast-occurring processes (either binding or conformational rearrangements) that lead to receptor signaling. Because of their rapid rate, these processes might reoccur each time immediately after the peptide dissociates from the receptor surface and before it can rebind. By remaining on the receptor surface for prolonged periods of time, AHNP analogues with low dissociation rates effectively block receptor activity. Our data suggest that high binding affinity does not necessarily have to be the main goal that determines the success of structure-based drug design. As we have shown for the AHNP mimetics, the dissociation rate constant can be a very important constituent of peptides' biological activity. Depending on a drug's mechanism of action, a slow k_{off} can compensate for low affinity in certain situations.

In summary, for a number of AHNP analogues, we were able to achieve significant improvements in receptor-binding affinity, solubility, or accessibility for labeling by introducing additional hydrophobic or polar groups. More importantly, the optimized analogues showed almost antibody-like dissociation rate constant, which, as we have shown in our structure−activity studies, is a critical activity-determining parameter for this class of peptides. Optimization of both entropic and enthalpic components of peptide-receptor binding, performed in this study, has significantly improved solubility and binding properties of antibody-derived peptides (including affinities and dissociation rate constants) while retaining the high specificity typical for a full-size antibody.

Experimental Section

Peptide Synthesis and Cyclization. Linear peptides (95% purity) were ordered from the Protein Chemistry Laboratory, University of Pennsylvania. Peptide purity and identity was confirmed by reverse phase high performance liquid chromatography (RP HPLC) and MALDI mass-spectrometry, using a time-of-flight mass spectrometer (MicroMass TofSpec; Micromass Inc., Beverly, Mass.). The peptides were cyclized by air oxidation in distilled water adjusted to pH 8.0 with $(NH_4)_2CO_3$ at 0.1 mg/mL and 4 °C. Progress of the oxidation was controlled by measuring amounts of free thiols with 5,5′-dithio-bis(2-nitrobenzoic) acid (DTNB). Briefly, 0.4 mL of an AHNP peptide (0.1 mg/mL) and 5 μL of DTNB (20 mM) were added to 0.2 mL of 0.1 M sodium phosphate buffer, pH 8.0. Absorbance at 412 nm was measured and compared with the linear unoxidized peptides. The cyclized peptides were lyophilized and their purity was analyzed by RP HPLC using a C18

semipreparative column (Waters, Milford, MA). Typically, purity of higher than 95% was obtained for the cyclized peptides. Aliquotes of 1 mM stock solutions have been prepared for each peptide and kept at −20 °C to be thawed prior to the binding or bioassay studies. Peptide concentrations were confirmed by UV spectrophotometry using extinction coefficients at 280 nm calculated for each peptide as described in ref 73.

Interaction Studies. Binding experiments were performed with the surface plasmon resonance based biosensor instrument Biacore 3000 (Biacore AB, Uppsala, Sweden) at 25 °C. Recombinant purified HER2 receptor composed of the ectodomain of HER2 fused to the Fc of human IgG was provided by Dr. Che Law, Xcyte Therapeutics, Seattle, WA. Immobilization of HER2 in the sensor surface was performed following the standard amine coupling procedure according to manufacturer's instructions. Briefly, 35 μL of a solution containing 0.2 M N-ethyl-N'-(dimethylaminopropyl) carbodiimide (EDC) and 0.05 M N-hydroxysuccinimide (NHS) were injected at a flow rate of 5 μL/min to activate carboxyl groups on the sensor chip surface. HER2 (40 ng/mL in 10 mM NaOAc buffer, pH 5.0) was flowed over the chip surface at a flow rate of 20 μL/min until the desired level bound protein was reached. Unreacted protein was washed out and unreacted activated groups were blocked by the injection of 35 μL of 1 M ethanolamine at 5 μL/min. The final immobilization response of HER2 was 3500 RU. A reference surface was generated simultaneously under the same conditions but without HER2 injection and used as a blank to correct for instrument and buffer artifacts. Peptides were injected at variable concentrations at 20 μL/min flow rate and binding to the HER2 receptor immobilized on the chip was monitored in real time. Each sensorgram consists of an association phase (first 240 s), reflecting binding of the injected peptide to the receptor, followed by a dissociation phase (300 s), during which the running buffer is passed over the chip and the bound peptide is being washed off the receptor surface. In competition studies, peptides were preinjected for 5 min at 20 mL/min at concentrations ranging from 0 to 90 μM. rhumAb 4D5 (Genentech) was then injected for 5 min at 1 nM concentration in the "Coinject" mode. A control cyclic peptide CD4·M was used in some studies and was shown to be no different than blank control.

FITC-Labeling of Peptides. Two milligrams of each peptide were dissolved in 1 mL of 0.02 M Na_2CO_3−$NaHCO_3$ buffer, pH 9.1, containing 0.02 M NaCl. A total of 0.5 mL of 1% (w/v) fluorescein 5-isothiocyanate (FITC) dissolved in methanol was added to the peptide solution, and the reaction mixture was incubated in the dark for 2 h at room temperature. The reaction was terminated by rapid passage of the reaction mixture through a Sephadex G-10 column equilibrated with isotonic phosphate-buffered saline, pH 7.4, and further purified by C18 reverse-phase HPLC. The purified FITC-labeled peptides were dried under vacuum. Peptide identity was confirmed by MALDI mass spectroscopy.

MTT Assay. The MTT assay has been used for measuring cell growth as previously described in ref 46. Briefly, T6-17 cells were seeded in 96-well plates overnight in DMEM containing 10% FBS (1000 per well). T6-17 is derived from NIH3T3 by overexpressing the human HER2 receptor. Cells were cultured in 100 μL of fresh medium containing 1 μg/mL of peptides for 48 h. This incubation time was optimal for measuring inhibitory effects of different analogues. No improvements in the inhibitory activity could be achieved by increasing the incubation period. A total of 25 μL of MTT solution (5 mg/mL in PBS) was added to each well, and after 2 h of incubation at 37 °C, 100 μL of the extraction buffer (20% w/v of SDS, 50% N,N-dimethyl formamide, pH 4.7) were added. After an overnight incubation at 37 °C, the optical density at 600 nm was measured using an ELISA reader.

Molecular Modeling. Molecular modeling of AHNP has been performed as described previously.[40] Other AHNP analogues were designed by comparative modeling using AHNP as a template. To that end, point mutations or deletions have been introduced in the AHNP sequence using the "Protein Design" application of program QUANTA (Molecular Simulation, MA). Each analogue has been evaluated for the backbone and side chain orientation and solvent effects using a combination of energy minimization (CHARMM) and molecular dynamics simulations at room temperature (300 °K) and at 600 °K. Low energy conformers were further minimized and compared with AHNP and the native conformation of the template CDR3 loop of rhumAb 4D5.

References

(1) Dougall, W. C.; Qian, X.; Peterson, N. C.; Miller, M. J.; Samanta, A.; et al. The neu-oncogene: signal transduction pathways, transformation mechanisms and evolving therapies. *Oncogene* **1994**, *9*, 2109−2123.

(2) Hynes, N. E.; Stern, D. F. The biology of erbB-2/neu/HER-2 and its role in cancer. *Biochim. Biophys. Acta* **1994**, *1198*, 165−184.

(3) Reese, D. M.; Slamon, D. J. HER-2/neu signal transduction in human breast and ovarian cancer. *Stem Cells* **1997**, *15*, 1−8.

(4) Alroy, I.; Yarden, Y. The ErbB signaling network in embryogenesis and oncogenesis: signal diversification through combinatorial ligand−receptor interactions. *FEBS Lett.* **1997**, *410*, 83−86.

(5) Klapper, L. N.; Kirschbaum, M. H.; Sela, M.; Yarden, Y. Biochemical and clinical implications of the ErbB/HER signaling network of growth factor receptors. *Adv. Cancer Res.* **2000**, *77*, 25−79.

(6) Drebin, J. A.; Link, V. C.; Greene, M. I. Monoclonal antibodies reactive with distinct domains of the neu oncogene-encoded p185 molecule exert synergistic antitumor effects in vivo. *Oncogene* **1988**, *2*, 273−277.

(7) O'Rourke, D. M.; Greene, M. I. Immunologic approaches to inhibiting cell-surface-residing oncoproteins in human tumors. *Immunol. Res.* **1998**, *17*, 179−189.

(8) Murali, R.; Greene, M. I. Structure-based design of immunologically active therapeutic peptides. *Immunol. Res.* **1998**, *17*, 163−169.

(9) O'Rourke, D. M.; Nute, E. J.; Davis, J. G.; Wu, C.; Lee, A. et al. Inhibition of a naturally occurring EGFR oncoprotein by the p185neu ectodomain: implications for subdomain contributions to receptor assembly. *Oncogene* **1998**, *16*, 1197−1207.

(10) O'Rourke, D. M.; Kao, G. D.; Singh, N.; Park, B. W.; Muschel, R. J.; et al. Conversion of a radioresistant phenotype to a more sensitive one by disabling erbB receptor signaling in human cancer cells. *Proc. Natl. Acad Sci. U.S.A.* **1998**, *95*, 10842−10847.

(11) Zhang, H.; Wang, Q.; Montone, K. T.; Peavey, J. E.; Drebin, J. A.; et al. Shared antigenic epitopes and pathobiological functions of anti-p185(her2/neu) monoclonal antibodies. *Exp. Mol. Pathol.* **1999**, *67*, 15−25.

(12) Wels, W.; Harwerth, I. M.; Mueller, M.; Groner, B.; Hynes, N. E. Selective inhibition of tumor cell growth by a recombinant single-chain antibody-toxin specific for the erbB-2 receptor. *Cancer Res.* **1992**, *52*, 6310−6317.

(13) Wels, W.; Harwerth, I. M.; Hynes, N. E.; Groner, B. Diminution of antibodies directed against tumor cell surface epitopes: a single chain Fv fusion molecule specifically recognizes the extracellular domain of the c-erbB-2 receptor. *J. Steroid Biochem. Mol. Biol.* **1992**, *43*, 1−7.

(14) Xu, F. J.; Boyer, C. M.; Bae, D. S.; Wu, S.; Greenwald, M.; et al. The tyrosine kinase activity of the C-erbB-2 gene product (p185) is required for growth inhibition by anti-p185 antibodies but not for the cytotoxicity of an anti-p185-ricin-A chain immunotoxin. *Int. J. Cancer* **1994**, *59*, 242−247.

(15) Weiner, L. M. An overview of monoclonal antibody therapy of cancer. *Semin. Oncol.* **1999**, *26*, 41−50.

(16) Sliwkowski, M. X.; Lofgren, J. A.; Lewis, G. D.; Hotaling, T. E.; Fendly, B. M.; et al. Nonclinical studies addressing the mechanism of action of trastuzumab (Herceptin). *Semin. Oncol.* **1999**, *26*, 60−70.

(17) Goldenberg, D. M.; Nabi, H. A. Breast cancer imaging with radiolabeled antibodies. *Semin. Nuclear Med.* **1999**, *29*, 41−48.

(18) Latham, P. W. Therapeutic peptides revisited. *Nat. Biotechnol.* **1999**, *17*, 755−757.

(19) Amit, A. G.; Mariuzza, R. A.; Phillips, S. E.; Poljak, R. J. Three-dimensional structure of an antigen−antibody complex at 2.8 A resolution. *Science* **1986**, *233*, 747−753.

(20) Bruck, C.; Co, M. S.; Slaoui, M.; Gaulton, G. N.; Smith, T.; et al. Nucleic acid sequence of an internal image-bearing monoclonal anti- idiotype and its comparison to the sequence of the external antigen. *Proc. Natl. Acad. Sci. U.S.A.* **1986**, *83*, 6578−6582.

(21) Williams, W. V.; Moss, D. A.; Kieber-Emmons, T.; Cohen, J. A.; Myers, J. N.; et al. Development of biologically active peptides based on antibody structure [published erratum appears in *Proc. Natl. Acad. Sci. U.S.A.* **1989** Oct; *86* (20), 8044]. *Proc. Natl. Acad. Sci. U.S.A.* **1989**, *86*, 5537−5541.

(22) Williams, W. V.; Kieber-Emmons, T.; VonFeldt, J.; Greene, M. I.; Weiner, D. B. Design of bioactive peptides based on antibody hypervariable region structures. Development of conformationally constrained and dimeric peptides with enhanced affinity. *J. Biol. Chem.* **1991**, *266*, 5182−5190.

(23) Dougall, W. C.; Peterson, N. C.; Greene, M. I. Antibody-structure-based design of pharmacological agents. *Trends Biotechnol.* **1994**, *12*, 372−379.

(24) Saragovi, H. U.; Fitzpatrick, D.; Raktabutr, A.; Nakanishi, H.; Kahn, M.; et al. Design and synthesis of a mimetic from an antibody complementarity- determining region. *Science* **1991**, *253*, 792−795.

(25) Takahashi, M.; Ueno, A.; Uda, T.; Mihara, H. Design of novel porphyrin-binding peptides based on antibody CDR. *Bioorg. Med. Chem. Lett.* **1998**, *8*, 2023−2026.

(26) Takahashi, M.; Ohgitani, Y.; Ueno, A.; Mihara, H. Design of peptides derived from anti-IgE antibody for allergic treatment. *Bioorg. Med. Chem. Lett.* **1999**, *9*, 2185−2188.

(27) Feng, Y.; Chung, D.; Garrard, L.; McEnroe, G.; Lim, D.; et al. Peptides derived from the complementarity-determining regions of anti- Mac-1 antibodies block intercellular adhesion molecule-1 interaction with Mac-1. *J. Biol. Chem.* **1998**, *273*, 5625−5630.

(28) Avrameas, A.; Ternynck, T.; Nato, F.; Buttin, G.; Avrameas, S. Polyreactive anti-DNA monoclonal antibodies and a derived peptide as vectors for the intracytoplasmic and intranuclear translocation of macromolecules. *Proc. Natl. Acad. Sci. U.S.A.* **1998**, *95*, 5601−5606.

(29) Chatterjee, S. K.; Tripathi, P. K.; Chakraborty, M.; Yannelli, J.; Wang, H.; et al. Molecular mimicry of carcinoembryonic antigen by peptides derived from the structure of an anti-idiotype antibody. *Cancer Res.* **1998**, *58*, 1217−1224.

(30) Deng, Y.; Notkins, A. L. Molecular determinants of polyreactive antibody binding: HCDR3 and cyclic peptides. *Clin. Exp. Immunol.* **2000**, *119*, 69−76.

(31) Jouanne, C.; Avrameas, S.; Payelle-Brogard, B. A peptide derived from a polyreactive monoclonal anti-DNA natural antibody can modulate lupus development in (NZBxNZW)F1 mice. *Immunology* **1999**, *96*, 333−339.

(32) Sivolapenko, G. B.; Douli, V.; Pectasides, D.; Skarlos, D.; Sirmalis, G.; et al. Breast cancer imaging with radiolabeled peptide from complementarity- determining region of antitumour antibody. *Lancet* **1995**, *346*, 1662−1666.

(33) Hussain, R.; Courtenay-Luck, N. S.; Siligardi, G. Structure−function correlation and biostability of antibody CDR-derived peptides as tumour imaging agents. *Biomed. Pept. Proteins Nucleic Acids* **1996**, *2*, 67−70.

(34) Monnet, C.; Laune, D.; Laroche-Traineau, J.; Biard-Piechaczyk, M.; Briant, L.; et al. Synthetic peptides derived from the variable regions of an anti-CD4 monoclonal antibody bind to CD4 and inhibit HIV-1 promoter activation in virus-infected cells. *J. Biol. Chem.* **1999**, *274*, 3789−3796.

(35) Waisman, A.; Ruiz, P. J.; Israeli, E.; Eilat, E.; Konen-Waisman, S.; et al. Modulation of murine systemic lupus erythematosus with peptides based on complementarity determining regions of a pathogenic anti-DNA monoclonal antibody. *Proc. Natl. Acad. Sci. U.S.A.* **1997**, *94*, 4620−4625.

(36) Laune, D.; Molina, F.; Ferrieres, G.; Mani, J. C.; Cohen, P.; et al. Systematic exploration of the antigen binding activity of synthetic peptides isolated from the variable regions of immunoglobulins. *J. Biol. Chem.* **1997**, *272*, 30937−30944.

(37) Igarashi, K.; Asai, K.; Kaneda, M.; Umeda, M.; Inoue, K. Specific binding of a synthetic peptide derived from an antibody complementarity determining region to phosphatidylserine. *J. Biochem. (Tokyo)* **1995**, *117*, 452−457.

(38) Brosh, N.; Dayan, M.; Fridkin, M.; Mozes, E. A peptide based on the CDR3 of an anti-DNA antibody of experimental SLE origin is also a dominant T-cell epitope in (NZBXNZW)F1 lupus-prone mice. *Immunol. Lett.* **2000**, *72*, 61−68.

(39) Brosh, N.; Eilat, E.; Zinger, H.; Mozes, E. Characterization and role in experimental systemic lupus erythematosus of T-cell lines specific to peptides based on complementarity- determining region-1 and complementarity-determining region-3 of a pathogenic anti-DNA monoclonal antibody. *Immunology* **2000**, *99*, 257−265.

(40) Park, B. W.; Zhang, H. T.; Wu, C.; Berezov, A.; Zhang, X.; et al. Rationally designed anti-HER2/neu peptide mimetic disables P185HER2/neu tyrosine kinases in vitro and in vivo. *Nat. Biotechnol.* **2000**, *18*, 194−198.

(41) Myszka, D. G. Improving biosensor analysis. *J. Mol. Recognit.* **1999**, *12*, 279−284.

(42) Myszka, D. G.; Jonsen, M. D.; Graves, B. J. Equilibrium analysis of high affinity interactions using BIACORE. *Anal. Biochem.* **1998**, *265*, 326−330.

(43) Canziani, G.; Zhang, W.; Cines, D.; Rux, A.; Willis, S.; et al. Exploring biomolecular recognition using optical biosensors. *Methods* **1999**, *19*, 253−269.

(44) Ober, R. J.; Ward, E. S. The influence of signal noise on the accuracy of kinetic constants measured by surface plasmon resonance experiments. *Anal. Biochem.* **1999**, *273*, 49−59.

(45) Downer, J. B.; McCarthy, T. J.; Edwards, W. B.; Anderson, C. J.; Welch, M. J. Reactivity of p-[18F]fluorophenacyl bromide for radiolabeling of proteins and peptides. *Appl. Radiat. Isot.* **1997**, *48*, 907−916.

(46) Hansen, M. B.; Nielsen, S. E.; Berg, K. Reexamination and further development of a precise and rapid dye method for measuring cell growth/cell kill. *J. Immunol. Methods* **1989**, *119*, 203-210.

(47) Karlsson, R. Real-time competitive kinetic analysis of interactions between low- molecular-weight ligands in solution and surface-immobilized receptors. *Anal. Biochem.* **1994**, *221*, 142−151.

(48) Karlsson, R.; Stahlberg, R. Surface plasmon resonance detection and multispot sensing for direct monitoring of interactions involving low-molecular-weight analytes and for determination of low affinities. *Anal. Biochem.* **1995**, *228*, 274−280.

(49) Gomes, P.; Giralt, E.; Andreu, D. Surface plasmon resonance screening of synthetic peptides mimicking the immunodominant region of C−S8c1 foot-and-mouth disease virus. *Vaccine* **1999**, *18*, 362−370.

(50) Gomes, P.; Giralt, E.; Andreu, D. Direct single-step surface plasmon resonance analysis of interactions between small peptides and immobilized monoclonal antibodies. *J. Immunol. Methods* **2000**, *235*, 101−111.

(51) Ploug, M.; Ostergaard, S.; Hansen, L. B.; Holm, A.; Dano, K. Photoaffinity labeling of the human receptor for urokinase-type plasminogen activator using a decapeptide antagonist. Evidence for a composite ligand-binding site and a short interdomain separation. *Biochemistry* **1998**, *37*, 3612−3622.

(52) Ohlson, S.; Strandh, M.; Nilshans, H. Detection and characterization of weak affinity antibody antigen recognition with biomolecular interaction analysis. *J. Mol. Recognit.* **1997**, *10*, 135−138.

(53) Piehler, J.; Brecht, A.; Gauglitz, G.; Maul, C.; Grabley, S.; et al. Specific binding of low molecular weight ligands with direct optical detection. *Biosens. Bioelectron.* **1997**, *12*, 531−538.

(54) Markgren, P. O.; Hamalainen, M.; Danielson, U. H. Screening of compounds interacting with HIV-1 proteinase using optical biosensor technology. *Anal. Biochem.* **1998**, *265*, 340−350.

(55) Markgren, P. O.; Hamalainen, M.; Danielson, U. H. Kinetic analysis of the interaction between HIV-1 protease and inhibitors using optical biosensor technology. *Anal. Biochem.* **2000**, *279*, 71−78.

(56) Strandh, M.; Persson, B.; Roos, H.; Ohlson, S. Studies of interactions with weak affinities and low-molecular-weight compounds using surface plasmon resonance technology. *J. Mol. Recognit.* **1998**, *11*, 188−190.

(57) Malmqvist, M. BIACORE: an affinity biosensor system for characterization of biomolecular interactions. *Biochem. Soc. Trans.* **1999**, *27*, 335−340.

(58) Kampranis, S. C.; Gormley, N. A.; Tranter, R.; Orphanides, G.; Maxwell, A. Probing the binding of coumarins and cyclothialidines to DNA gyrase. *Biochemistry* **1999**, *38*, 1967−1976.

(59) Yamashita, D. S.; Smith, W. W.; Zhao, B.; Janson, C. A.; Tomaszek, T. A.; Bossard, M. J.; Levy, M. A.; Oh, H.-J.; Carr, T. J.; Thompson, S. K.; Ijames, C. F.; Carr, S. A.; McQueney, M.; D'Alessio, K. J.; Amegadzie, B. Y.; Hanning, C. R.; Abdel-Meguid, S.; DesJarlais, R. L.; Gleason, J. G.; Veber, D. F. Structure and design of potent and selective Cathepsin K Inhibitors. *J. Am. Chem. Soc.* **1997**, *119*, 11351−11352.

(60) Thompson, S. K.; Halbert, S. M.; Bossard, M. J.; Tomaszek, T. A.; Levy, M. A.; et al. Design of potent and selective human cathepsin K inhibitors that span the active site. *Proc. Natl. Acad. Sci. U.S.A.* **1997**, *94*, 14249−14254.

(61) McGrath, M. E.; Klaus, J. L.; Barnes, M. G.; Bromme, D. Crystal structure of human cathepsin K complexed with a potent inhibitor [letter]. *Nat. Struct. Biol.* **1997**, *4*, 105−109.

(62) Turk, D.; Podobnik, M.; Popovic, T.; Katunuma, N.; Bode, W.; et al. Crystal structure of cathepsin B inhibited with CA030 at 2.0-A resolution: A basis for the design of specific epoxysuccinyl inhibitors. *Biochemistry* **1995**, *34*, 4791−4797.

(63) Yamamoto, D.; Matsumoto, K.; Ohishi, H.; Ishida, T.; Inoue, M.; et al. Refined X-ray structure of papain. E-64-c complex at 2.1-A resolution. *J. Biol. Chem.* **1991**, *266*, 14771−14777.
(64) Sautel, M.; Rudolf, K.; Wittneben, H.; Herzog, H.; Martinez, R.; et al. Neuropeptide Y and the nonpeptide antagonist BIBP 3226 share an overlapping binding site at the human Y1 receptor. *Mol. Pharmacol.* **1996**, *50*, 285−292.
(65) Schwartz, T. W. Locating ligand-binding sites in 7TM receptors by protein engineering. *Curr. Opin. Biotechnol.* **1994**, *5*, 434−444.
(66) Ripka, A. S.; Rich, D. H. Peptidomimetic design. *Curr. Opin. Chem. Biol.* **1998**, *2*, 441−452.
(67) Meyer, E. F.; Botos, I.; Scapozza, L.; Zhang, D. Backward binding and other structural surprises. *Perspect. Drug Discovery Des.* **1995**, *3*, 168−195.
(68) Sheriff, S.; Silverton, E. W.; Padlan, E. A.; Cohen, G. H.; Smith-Gill, S. J.; et al. Three-dimensional structure of an antibody−antigen complex. *Proc. Natl. Acad. Sci. U.S.A.* **1987**, *84*, 8075−8079.
(69) Padlan, E. A.; Silverton, E. W.; Sheriff, S.; Cohen, G. H.; Smith-Gill, S. J.; et al. Structure of an antibody−antigen complex: crystal structure of the HyHEL-10 Fab-lysozyme complex. *Proc. Natl. Acad. Sci. U.S.A.* **1989**, *86*, 5938−5942.
(70) Leysen, J. E.; Gommeren, W. The dissociation rate of unlabeled dopamine antagonists and agonists from the dopamine-D2 receptor, application of an original filter method. *J. Recept. Res.* **1984**, *4*, 817−845.
(71) Pargellis, C. A.; Morelock, M. M.; Graham, E. T.; Kinkade, P.; Pav, S.; et al. Determination of kinetic rate constants for the binding of inhibitors to HIV-1 protease and for the association and dissociation of active homodimer. *Biochemistry* **1994**, *33*, 12527−12534.
(72) Frieden, C.; Kurz, L. C.; Gilbert, H. R. Adenosine deaminase and adenylate deaminase: comparative kinetic studies with transition state and ground-state analogue inhibitors. *Biochemistry* **1980**, *19*, 5303−5309.
(73) Gill, S. C.; von Hippel, P. H. Calculation of protein extinction coefficients from amino acid sequence data. *Anal. Biochem.* **1989**, *182*, 319−326.

JM000527M